# UC Berkeley

## UC Berkeley Previously Published Works


### Title

Anomalous Anderson localization behaviors in disordered pseudospin systems


### Permalink

https://escholarship.org/uc/item/7695s1wc



### Journal

Proceedings of the National Academy of Sciences of the United States of America, 114(16)

### ISSN

0027-8424



### Authors

Fang, A
Zhang, ZQ
Louie, Steven G
et al.



### Publication Date

2017-04-18

### DOI

10.1073/pnas.1620313114

Peer reviewed



eScholarship.org Powered by the California Digital Library
University of California

# Anomalous Anderson localization behaviors in disordered pseudospin systems

A. Fang[a,b], Z. Q. Zhang[a,b], Steven G. Louie[b,c,d], and C. T. Chan[a,b,1]

[a]Department of Physics, The Hong Kong University of Science and Technology, Clear Water Bay, Hong Kong, China; [b]Institute for Advanced Study, The Hong Kong University of Science and Technology, Clear Water Bay, Hong Kong, China; [c]Department of Physics, University of California, Berkeley, CA 94720; and [d]Materials Sciences Division, Lawrence Berkeley National Laboratory, Berkeley, CA 94720

Edited by David A. Weitz, Harvard University, Cambridge, MA, and approved March 7, 2017 (received for review December 11, 2016)

**We discovered unique Anderson localization behaviors of pseudospin systems in a 1D disordered potential. For a pseudospin-1 system, due to the absence of backscattering under normal incidence and the presence of a conical band structure, the wave localization behaviors are entirely different from those of conventional disordered systems. We show that there exists a critical strength of random potential ($W_c$), which is equal to the incident energy ($E$), below which the localization length $\xi$ decreases with the random strength $W$ for a fixed incident angle $\theta$. But the localization length drops abruptly to a minimum at $W = W_c$ and rises immediately afterward. The incident angle dependence of the localization length has different asymptotic behaviors in the two regions of random strength, with $\xi \propto \sin^{-4}\theta$ when $W < W_c$ and $\xi \propto \sin^{-2}\theta$ when $W > W_c$. The existence of a sharp transition at $W = W_c$ is due to the emergence of evanescent waves in the systems when $W > W_c$. Such localization behavior is unique to pseudospin-1 systems. For pseudospin-1/2 systems, there is also a minimum localization length as randomness increases, but the transition from decreasing to increasing localization length at the minimum is smooth rather than abrupt. In both decreasing and increasing regions, the $\theta$ dependence of the localization length has the same asymptotic behavior $\xi \propto \sin^{-2}\theta$.**

localization | pseudospin | disorder | evanescent waves | photonic crystals

Anderson localization is one of the most fundamental and universal phenomena in disordered systems. Anderson's seminal work (1) has inspired intensive studies on the effect of randomness in a vast variety of electronic and classical wave systems (2–10). Meanwhile, the rapid progress in experimental techniques enables us to reach an unprecedented level of manipulating artificial materials such as ultracold atomic gases (11) and nano/microdielectric structures (12), making it possible to create new materials with unusual transport properties (11–14). The interplay between disorder and new artificial materials continues to generate many amazing phenomena, such as the suppression of Anderson localization in metamaterials (15–17), supercollimation of electron beams in 1D disorder potentials (18), and delocalization of relativistic Dirac particles in 1D disordered systems (19).

Among these new materials, pseudospin-1/2 materials are of particular interest due to their conical band structure and the chiral nature of the underlying quasiparticle states. A prototypical example of such materials is graphene (13, 14). The low-energy excitations in graphene behave like massless Dirac particles and the orbital wave function can be represented by a two-component spinor, with each component corresponding to the amplitude of the electron wave function on one of the trigonal sublattices of graphene. We emphasize that the "pseudospin-1/2" character in graphene refers to the spatial degree of freedom and has nothing to do with the intrinsic spin of electrons. The Dirac cone and the associated pseudospin-1/2 characteristic of quasiparticles can also be found in a wide range of quantum and classical wave systems, such as topological insulators (20, 21) and the photonic and phononic counterparts of graphene (22–24). Recently, pseudospin-1 systems have also attracted much attention (23–38). Different from the Dirac cones in graphene, a Dirac-like cone is found in pseudospin-1 systems where two cones meet and intersect with an additional flat band at a Dirac-like point. For example, certain photonic crystals (PCs) can exhibit such conical dispersions at the Brillouin zone center due to the accidental degeneracy of monopole and dipole excitations (23–27), which combines to give three degrees of freedom. The physics near the Dirac-like point can be described by an effective spin-orbit Hamiltonian with pseudospin $S = 1$ and their wave functions are represented by a three-component spinor. Such systems are called "pseudospin-1 materials" (27). These systems have also been theoretically predicted (28–32) and experimentally realized by manipulating ultracold atoms in an optical lattice (33) or arranging an array of optical waveguides in a Lieb lattice (34–37). As an analogy with the gate voltage in graphene and other charged Dirac fermion systems, the potentials in pseudospin-1 systems can be shifted up and down by a simple change of length scale in PCs (27) or an appropriate holographic mask in ultracold atom systems (28–32).

Whereas these pseudospin Hamiltonians share the common feature of conical dispersions near a singular point, different pseudospin numbers (1 vs. 1/2) give rise to distinct physical behaviors. For example, carriers in pseudospin-1/2 systems encircling the Dirac point pick up a Berry phase of $\pi$ whereas those in pseudospin-1 systems pick up a Berry phase of 0 (14, 27),

## Significance

**Wave propagation through a 1D disordered potential is always confined spatially due to the constructive interference in the backward direction. This "Anderson localization" behavior applies to all previously known 1D disordered systems in nature. Here, we show that wave propagating in 2D pseudospin-1 systems with 1D disorder has unique localization behaviors. In all conventional materials, stronger disorder always induces stronger localization. However, the localization in pseudospin-1 systems actually becomes weaker after the randomness increases beyond a critical value and a sharp transition separates the localization behavior into two regimes with different localization characteristics. Pseudospin-1 systems have been achieved in artificial crystals such as metamaterials and ultracold atom systems, which would be interesting platforms to observe the anomalous localization behaviors.**

Author contributions: A.F., Z.Q.Z., S.G.L., and C.T.C. designed research; A.F. performed research; and A.F., Z.Q.Z., S.G.L., and C.T.C. wrote the paper.

The authors declare no conflict of interest.

This article is a PNAS Direct Submission.

[1]To whom correspondence should be addressed. Email: phchan@ust.hk.

This article contains supporting information online at www.pnas.org/lookup/suppl/doi:10.1073/pnas.1620313114/-/DCSupplemental.

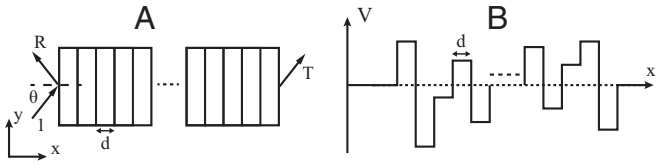


**Fig. 1.** Schematic diagram of 1D disordered systems. (*A*) Top view of the structure. Each layer has the same thickness *d*, but feels a randomized potential. (*B*) One possible realization of random potentials. The potentials *V* are uniformly distributed in the range $[-W, W]$.

meaning that the topological characteristics of the wave functions in momentum space depend on the pseudospin numbers and the localization behaviors may be different. In addition, in the presence of a 2D potential barrier, scattering of low-energy carriers in pseudospin-1/2 systems gives zero backscattering amplitude, whereas the scattering is isotropic for pseudospin-1 systems (38). The scattering behavior in the presence of a 1D potential barrier is also different. For example, the so-called "super-Klein tunneling" (perfect transmission for all incident angles when the incident energy equals half of the barrier) can exist only in pseudospin-1 systems (27–32). In 1D disordered graphene superlattices, localization behaviors such as angle-dependent electron transmission (39, 40) and directional filtering due to strong angle-dependent localization length (41) have been predicted. We present here some surprising, counterintuitive transport phenomena for pseudospin-1 systems in 1D disordered potentials (Fig. 1). We also show results of pseudospin-1/2 systems for comparison.

The disorder-induced localization behavior in pseudospin-1 systems under 1D disordered potentials is entirely different from that in any conventional disordered systems, in which all states become localized in 1D random potentials due to the constructive interference of two counterpropagating waves in the backward direction (2–5). However, for pseudospin-1 systems, a disordered 1D potential gives rise to a random phase only in the spatial wave function and does not produce any backward scatterings for waves propagating in the normal direction. Such behavior was first discovered in pseudospin-1/2 systems (14, 19, 42, 43). In the case of pseudospin-1 electromagnetic (EM) waves (27), the absence of backscattering can be interpreted as the impedance match between any two adjacent layers in such systems. Thus, Anderson localization occurs only for obliquely incident waves. It is interesting to point out that for conventional random layered media the impedance matching condition can also lead to a diverging localization length for p waves at some incident angle known as the stochastic Brewster effect (44, 45).

Furthermore, due to the existence of a Dirac-like point, the introduction of a disorder potential makes it possible to have evanescent waves occurring in the system when the potential at a certain layer is close to the incident energy. The presence of evanescent waves also makes the transport of waves different from that in conventional disordered systems. Here we show both analytically and numerically that, for pseudospin-1 systems, when the randomness is small so that no evanescent waves occur in any layer, the localization length $\xi$ decays with the incident angle $\theta$ according to $\xi \propto \sin^{-4}\theta$ at small $\theta$. However, when the strength of the random potential reaches a critical value, which equals the incident energy of the wave, the localization length drops suddenly to a minimum and rises immediately afterward as evanescent waves emerge. In the latter case, the $\theta$ dependence of $\xi$ changes to a different behavior; i.e., $\xi \propto \sin^{-2}\theta$. The sudden drop as well as the subsequently immediate rise of $\xi$ with increasing randomness and the change of the asymptotic behavior in the $\theta$ dependence are not seen in any conventional disordered systems, to the best of our knowledge (Fig. 2). In conventional disordered systems, $\xi$ always decreases with increasing randomness, consistent with our intuition that disorder should disrupt transmission. The existence of a critical randomness in pseudospin-1 systems suggests some kind of sharp transition between two localization phases. The physical origin of such a transition is the occurrence of evanescent waves in certain fluctuating layers with randomness that is beyond the critical randomness. Evanescent waves are known to produce a diffusive-like transport in an ordered graphene at the Dirac point (46, 47). We discover that evanescent waves can produce even more fascinating transport behaviors in disordered pseudospin-1 systems. For pseudospin-1/2 systems in 1D disordered potentials, our results find a smooth crossover in the localization length behavior, from a decreasing one at small randomness to an increasing one at large randomness, and an angular dependence of $\xi \propto \sin^{-2}\theta$ in both the localization length decreasing and increasing regimes. We show that the absence of the sharp transition in pseudospin-1/2 systems is due to the presence of additional interface scatterings, which produces a $\xi \propto \sin^{-2}\theta$ behavior even at small randomness. Thus, the $\theta$-dependent localization length behavior does not change when the randomness is increased.

## Results and Discussion

**Models and Numerical Results.** The systems under investigation are pseudospin-1 systems in 1D disordered potentials, which are in the form of $N$ random layers (or strips). Each layer has the same thickness $d$, but feels a random potential $V(x)$ with a strength $W$, as shown in Fig. 1. Here, $V = 0$ denotes the energy of the Dirac-like point of the background medium. A plane wave is incident on the layered structure at an incident angle $\theta$ from the background with the incident energy $E$. For normal incidence ($\theta = 0$), the waves are delocalized, irrespective of the strength of randomness due to the absence of backscattering (27). Here we consider oblique incidence ($\theta \neq 0$), for which

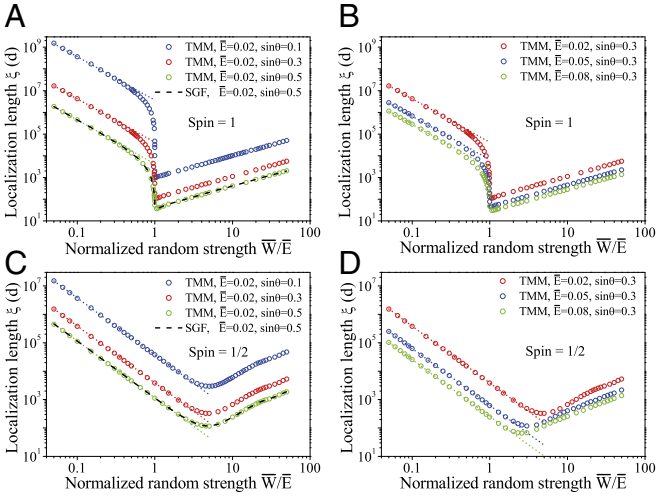


**Fig. 2.** Localization length as a function of normalized random potential strength for different incident angles and energies in 1D disordered pseudospin-1 and -1/2 systems calculated with the TMM. (*A*) Localization length for three different incident angles in pseudospin-1 systems. (*B*) Localization length for three different incident energies in pseudospin-1 systems. (*C*) Same as *A*, but for pseudospin-1/2 systems. (*D*) Same as *B*, but for pseudospin-1/2 systems. The black dashed lines in *A* and *C* show the results obtained by the surface Green function (SGF) method. The localization lengths for small $\overline{W}$ are fitted by dotted lines, showing an asymptotic behavior $\xi \propto \overline{W}^{-2}$. Both $\overline{E}$ and $\overline{W}$ are in units of $2\pi/d$.

Anderson localization can occur. It has been shown previously that the wave equation of such systems can be described by a generalized 2D Dirac equation with a 1D random potential (27–32),

$$H\psi = [\hbar v_g \vec{\mathrm{S}} \cdot \vec{\mathrm{k}} + V(x)\mathrm{I}]\psi = E\psi. \quad [1]$$

Here $\psi$ is a spinor function, $\vec{\mathrm{k}} = (k_x, k_y)$ is the wavevector operator with $k_x = -i\frac{\partial}{\partial x}$ and $k_y = -i\frac{\partial}{\partial y}$, $\vec{\mathrm{S}} = (S_x, S_y)$ is the matrix representation of the spin-1 operator, $v_g$ is the group velocity, and I is the identity matrix in the pseudospin space. We note that Eq. **1** is valid for both matter waves (quantum particles) (28–32) and EM waves (27) as long as the dispersion of the system near some high-symmetry k points can be described by the pseudospin-1 model. For simplicity, Eq. **1** can be rewritten as

$$[\vec{\mathrm{S}} \cdot \vec{\mathrm{k}} + \overline{V}(x)\mathrm{I}]\psi = \overline{E}\psi, \quad [2]$$

with $\overline{E} = E/\hbar v_g$ and $\overline{V}(x) = V(x)/\hbar v_g$. The normalized random potential in the $j$th layer is taken to be $\overline{V}(x) = \overline{\mathrm{v}}_j$ ($j = 1, 2, 3, \cdots, N$), which is an independent random variable distributed uniformly in the range $[-\overline{W}, \overline{W}]$ ($\overline{W} = W/\hbar v_g$ is the random strength of the normalized potential). We can calculate the transmission coefficient $T_N$ through a random stack of $N$ layers by the transfer-matrix method (TMM) (27). The localization length $\xi$, or the inverse of the Lyapunov exponent $\gamma$, is obtained through the relation

$$\xi = \gamma^{-1} = -\lim_{N\to\infty} \frac{2Nd}{\langle \ln T_N \rangle_c}, \quad [3]$$

where $\langle\rangle_c$ denotes ensemble averaging.

We first show the localization length as a function of the random strength $\overline{W}$. Results of averaging over 4,000 configurations with $N$ taken to be five times the localization length are shown in Fig. 2 *A* and *B* for different incident angles and energies, respectively. At small randomness, these results show that the localization length decreases with increasing randomness following a general form $\xi \propto \overline{W}^{-2}$, similar to the behavior found in ordinary disordered media (3, 4). However, if $\overline{W}$ is further increased, the localization length $\xi$ drops abruptly to a minimum at a critical $\overline{W}_c = \overline{E}$, independent of incident angle and energy, and rises immediately afterward.

These results are rather intriguing. First, the cusp-like turnaround of localization behavior is not seen in any other disorder systems to our knowledge. For conventional disordered media, $\xi$ always decreases with increasing disorder. Second, the sudden change of localization behavior near the critical random strength $\overline{W}_c = \overline{E}$ indicates some kind of sharp transition between two different localization phases: $\overline{W} < \overline{E}$ and $\overline{W} > \overline{E}$ in the $\overline{E} - \overline{W}$ space. To further elaborate on this point, we examine the $\theta$ dependence of the localization length. The result of $\overline{E} = 0.02$ and small disorder $\overline{W} = 0.01$ ($<\overline{E}$) is shown by blue circles in Fig. 3*A*, where a log-log plot of $\xi$ vs. $\sin\theta$ shows a straight line with a slope of $-4$ for small incident angles $\theta$, indicating a $\xi \propto \sin^{-4}\theta$ behavior. However, the slope changes to $-2$ for a higher disorder $\overline{W} = 0.03$ ($>\overline{E}$) (blue diamonds), indicating a $\xi \propto \sin^{-2}\theta$ behavior. There is hence a change of localization behaviors from $\xi \propto \sin^{-4}\theta$ to $\xi \propto \sin^{-2}\theta$ in the two different regions of $\overline{W}$. We show analytically later that this transition occurs exactly at $\overline{W} = \overline{E}$, and the physical origins of the above anomalous localization behaviors are the existence of the Dirac-like point and the occurrence of evanescent waves in some layers caused by a diverging scattering strength when $\overline{W} > \overline{E}$.

To see whether such anomalous localization behaviors also occur in pseudospin-1/2 systems, we studied numerically the localization length behaviors for such systems. The Hamiltonian of pseudospin-1/2 systems has the same form as Eq. **1** except that the wave function is a two-component spinor (14, 18) and the spin matrices become Pauli matrices. The results of the TMM are shown in Fig. 2 *C* and *D*. Compared with Fig. 2 *A* and *B*, for all incident angles and energies studied, the cusp-like sharp change in $\xi$ does not exist in pseudospin-1/2 systems. Instead, $\xi$ shows a smooth crossover from a decreasing behavior at small randomness to an increasing one at large randomness with a minimum around a few $\overline{E}$. Furthermore, the $\theta$ dependence of $\xi$ in both regions shows a $\xi \propto \sin^{-2}\theta$ behavior as shown in Fig. 3*A*. The difference in the $\theta$ dependence of $\xi$ in the two pseudospin systems is due to different scattering potentials for oblique waves. In the following, we present analytical derivations of the localization length for both systems.

**Transformation from a Vector Wave Equation to a Scalar One.** For the layered structure, the wavevector component parallel to the interface ($k_y = k_0 \sin\theta$, where $k_0 = \overline{E}$ is the wavevector in the background) is conserved, with the same $k_y$ value in all layers. Thus, the wave functions for pseudospin-1 systems can be written as $\psi(x, y) = (\psi_1(x), \psi_2(x), \psi_3(x))^T e^{ik_y y}$. Using the following matrix representation for the spin operator, $\vec{\mathrm{S}} = S_x\hat{x} + S_y\hat{y}$,

$$S_x = \frac{1}{\sqrt{2}}\begin{pmatrix} 0 & 1 & 0 \\ 1 & 0 & 1 \\ 0 & 1 & 0 \end{pmatrix}, \quad S_y = \frac{1}{\sqrt{2}}\begin{pmatrix} 0 & -i & 0 \\ i & 0 & -i \\ 0 & i & 0 \end{pmatrix}, \quad [4]$$

we rewrite Eq. **2** as

$$\frac{1}{\sqrt{2}}\begin{pmatrix} 0 & -i\frac{\partial}{\partial x} - ik_y & 0 \\ -i\frac{\partial}{\partial x} + ik_y & 0 & -i\frac{\partial}{\partial x} - ik_y \\ 0 & -i\frac{\partial}{\partial x} + ik_y & 0 \end{pmatrix}\begin{pmatrix} \psi_1 \\ \psi_2 \\ \psi_3 \end{pmatrix} + \overline{V}(x)\begin{pmatrix} \psi_1 \\ \psi_2 \\ \psi_3 \end{pmatrix} = \overline{E}\begin{pmatrix} \psi_1 \\ \psi_2 \\ \psi_3 \end{pmatrix}. \quad [5]$$

By eliminating $\psi_1(x)$ and $\psi_3(x)$, we can convert Eq. **5** into a scalar wave equation for $\psi_2(x)$,

$$-\frac{d}{dx}\left(\frac{1}{\overline{E} - \overline{V}(x)}\frac{d\psi_2}{dx}\right) + \frac{k_y^2}{\overline{E} - \overline{V}(x)}\psi_2 = (\overline{E} - \overline{V}(x))\psi_2. \quad [6]$$

Without loss of generality, we take the first interface of the $N$-layer system as the origin, define a new dimensionless

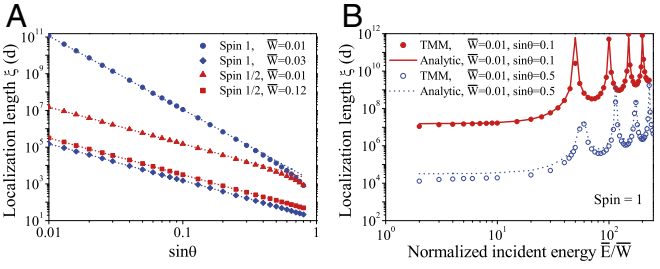


**Fig. 3.** Localization behaviors for disordered pseudospin-1 and -1/2 systems. (*A*) Localization length as a function of incident angle for incident energy $\overline{E} = 0.02$ and two random strengths in 1D disordered pseudospin-1 and -1/2 systems calculated using the TMM. The two random strengths are chosen from the respective decreasing and increasing regions in Fig. 2 *A* and *C* for pseudospin-1 and -1/2 systems. The localization length of pseudospin-1 systems at small $\theta$ for $\overline{W} = 0.01$ ($<\overline{E}$) (blue circles) is fitted by a dotted line, showing $\xi \propto \sin^{-4}\theta$. The other three cases are fitted by $\xi \propto \sin^{-2}\theta$. (*B*) Comparison of the localization length calculated by using the TMM and analytical results shown in Eq. **14**. Both $\overline{E}$ and $\overline{W}$ are in units of $2\pi/d$.

coordinate variable $u \equiv \int_0^x (\overline{E} - \overline{V}(x))dx$, and write $\Psi(u) \equiv \psi_2(x)$ and $\overline{U}(u) \equiv \overline{V}(x)$. Then, Eq. **6** can be reexpressed as

$$\frac{d^2\Psi}{du^2} + \Psi = \frac{k_y^2}{\left(\overline{E} - \overline{U}(u)\right)^2}\Psi. \quad [7]$$

The above coordinate transformation changes a nonstandard wave equation, Eq. **6**, to a standard one, Eq. **7**, where the scattering potential due to the disordered potential $V(x)$ is explicitly shown on the right-hand side of Eq. **7**. In the case of normal incidence, i.e., $k_y = 0$, Eq. **7** describes wave propagation in a homogeneous medium and contains two general solutions $\Psi \propto e^{\pm iu} = \exp\left[\pm i \int_0^x (\overline{E} - \overline{V}(x))dx\right]$. Thus, the accumulated random phase due to $V(x)$ during the one-way transport is now absorbed in the new coordinate $u$. For the layered structure where the potential is piecewise constant, the $i$th interface in the $u$ coordinate, $u_i$, is written as $u_1 = 0$ and $u_i = \sum_{j=1}^{i-1}(\overline{E} - \bar{v}_j)d$ for $i \geq 2$ from the above coordinate transformation. It is important to point out that we have transformed a three-component vector wave equation for obliquely propagating waves, i.e., Eq. **1**, into an equivalent scalar wave equation for normally propagating waves, and the oblique angle enters the wave equation in the scattering terms, i.e., Eq. **7**. Such a transformation allows us to derive analytically certain asymptotic localization behaviors.

Similarly, we can use the Pauli matrices for the spin-1/2 operator in Eq. **1** to construct a scalar wave equation for pseudospin-1/2 systems. In the $u$ coordinate system, the wave equation has the form (*Scalar Wave Equation*)

$$\frac{d^2\Psi}{du^2} + \Psi = \frac{k_y^2}{\left(\overline{E} - \overline{U}(u)\right)^2}\Psi + k_y\Psi\sum_{i=1}^{N+1} U_i\delta(u - u_i), \quad [8]$$

where $U_i = \frac{1}{\overline{E} - \bar{v}_i} - \frac{1}{\overline{E} - \bar{v}_{i-1}}$. Note that in comparison with pseudospin-1 systems, pseudospin-1/2 systems have additional interface scattering terms $k_y\Psi\sum_{i=1}^{N+1} U_i\delta(u - u_i)$ located at all $N + 1$ interfaces.

The difference in the $\theta$ dependence of $\xi$ in the two systems shown in Fig. 3*A*, when $\overline{W}$ is small, can be qualitatively understood from the scattering terms in Eqs. **7** and **8**. For ordinary disordered media, it is well accepted that the localization length in 1D systems is on the order of the mean free path, which is inversely proportional to the square of the scattering strength (3). In the case of small $k_y$, the $k_y^2$ dependence in the effective scattering potential of Eq. **7** gives rise to a $k_y^{-4}$ (or $\sin^{-4}\theta$) behavior in the localization length, whereas the $k_y$ dependence in the interface scattering terms of Eq. **8** dominates and leads to a $k_y^{-2}$ (or $\sin^{-2}\theta$) behavior. The sudden drop of localization length near $\overline{W} = \overline{E}$ for pseudospin-1 systems is due to the diverging scattering term in Eq. **7** when $|\overline{E} - \overline{U}(u)| < |k_y|$ in some layers so that the waves become evanescent inside those layers. We show analytically that it is the existence of those evanescent waves that changes the $\theta$ dependence of $\xi$ from $\xi \propto \sin^{-4}\theta$ in the region $\overline{W} < \overline{E}$ to $\xi \propto \sin^{-2}\theta$ in the region $\overline{W} > \overline{E}$. When $\overline{W}$ goes beyond its critical value $\overline{E}$, the probability of having evanescent waves is reduced with increasing $\overline{W}$, and in the meantime, the scattering potentials in the propagating layers are weakened in general. As a result, $\xi$ increases with $\overline{W}$. However, such a sudden drop of $\xi$ is smeared out by the interface scattering terms in Eq. **8** so that a smooth change of localization behaviors is found for pseudospin-1/2 systems.

**Lyapunov Exponent Obtained by the SGF Method.** Because Eqs. **7** and **8** are already in the form of scalar wave equations for normal-incident propagating waves, we can now solve the wave localization problem of pseudospin systems using the SGF method, which gives the following expression for the transmission coefficient of a normal-incident plane wave propagating through an $N$-layered random system (48):

$$T_N = |D_{N+1}|^{-2}, \quad [9]$$

where

$$\frac{D_{N+1}}{D_{N+1}^0} = \left[e^{2i\Phi_{1,N+1}}\prod_{n=1}^{N+1}(1 - r_{n,n-1})(1 - r_{n-1,n})\right]^{-\frac{1}{2}}. \quad [10]$$

Here $r_{n,n-1}$ denotes the reflection amplitude of a plane wave incident from the $n$th layer on the $(n-1)$th layer, $\Phi_{i,j} = \Phi_{j,i}$ is the phase accumulation between the $i$th and $j$th interfaces of the sample, and $D_{N+1}^0$ is the determinant of an $N + 1$ by $N + 1$ matrix $\hat{D}_{N+1}^0$ with the following elements:

$$\left(\hat{D}_{N+1}^0\right)_{nk} = \begin{cases} \delta_{nk} + (1 - \delta_{nk})r_{k,k-1}e^{i\Phi_{n,k}} & n \geq k, \\ \delta_{nk} + (1 - \delta_{nk})r_{k-1,k}e^{i\Phi_{n,k}} & n \leq k. \end{cases} \quad [11]$$

The expressions for $\Phi_{n,k}$ and $r_{k,k-1}$ are shown in *Phase Accumulation and Reflection Amplitudes* for both pseudospin-1 and -1/2 systems. From Eqs. **9** and **10**, we obtain the expression for Lyapunov exponent $\gamma$ in Eq. **3** as

$$\gamma = \xi^{-1} = \gamma_1 + \gamma_2, \quad [12]$$

with $\gamma_2 \equiv -\frac{1}{2Nd}\left\langle \ln\left|e^{2i\Phi_{1,N+1}}\prod_{n=1}^{N+1}(1 - r_{n,n-1})(1 - r_{n-1,n})\right|\right\rangle_c$ and $\gamma_1 \equiv \frac{1}{Nd}\left\langle \ln|D_{N+1}^0|\right\rangle_c$. We first numerically calculate the localization length by using Eq. **12** as a function of $\overline{W}$ for a fixed incident angle and energy. The results are shown as black dashed lines in Fig. 2 *A* and *C* for pseudospin-1 and -1/2 systems, respectively. They are in excellent agreement with those obtained from the TMM.

**Asymptotic $\theta$-Dependent Localization Length Behavior in Region $\overline{W} < \overline{E}$.** In the following, using Eq. **12**, we show analytically that localization length follows the asymptotic behavior $\xi \propto \sin^{-4}\theta$ in the region of $\overline{W} < \overline{E}$. In this case, the reflection amplitudes in pseudospin-1 systems can be approximated as $r_{n-1,n} = -r_{n,n-1} \approx -\frac{k_y^2}{4}\left[\frac{1}{(\overline{E} - \bar{v}_n)^2} - \frac{1}{(\overline{E} - \bar{v}_{n-1})^2}\right]$, as long as $|k_y| \ll |\overline{E} - \overline{U}(u)|$. In this limit, as shown in *Lyapunov Exponent in the Region of $\overline{W} < \overline{E}$*, the Lyapunov exponent $\gamma$ can be written as

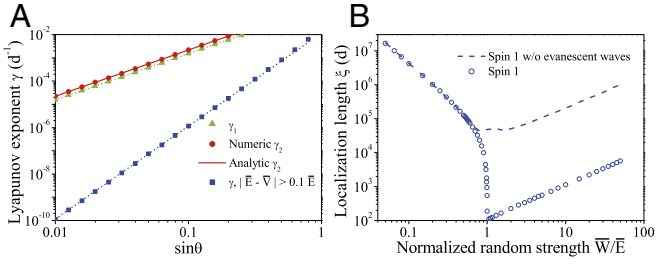


**Fig. 4.** Effect of evanescent waves on the localization behaviors in pseudospin-1 systems. (*A*) Comparison of the Lyapunov exponents as a function of incident angle with and without evanescent waves included in 1D disordered pseudospin-1 systems at $\overline{E} = 0.02$ and $\overline{W} = 0.03$. In the case with evanescent waves, $\gamma_1$ at small $\theta$ (green triangles) is fitted by a dotted line showing $\gamma_1 \propto \sin^2\theta$, and the numerical result of $\gamma_2$ (red circles) agrees excellently with the analytic prediction in Eq. **16** (red solid line). For the random distribution of potentials $|\overline{E} - \bar{v}| > 0.1\overline{E}$, no evanescent waves occur at sufficiently small $\theta$. $\gamma$ in this case (blue squares) shows an excellent fit to a dotted line $\gamma \propto \sin^4\theta$ for small $\theta$. (*B*) Comparison between the localization lengths with and without evanescent waves for pseudospin-1 systems with $\overline{E} = 0.02$ and $\sin\theta = 0.3$. Both $\overline{E}$ and $\overline{W}$ are in units of $2\pi/d$.

$$\gamma = \xi^{-1} = \gamma_1 + \gamma_2 \approx \frac{\overline{E}^4 \sin^4\theta}{32d}(\alpha_1 + \alpha_2), \qquad [13]$$

where $\alpha_1$ and $\alpha_2$ are coefficients corresponding to $\gamma_1$ and $\gamma_2$, respectively. Note that $\gamma$ in Eq. **13** is proportional to $\sin^4\theta$ for the region $\overline{W} < \overline{E}$. In the case of $\overline{W} \ll \overline{E}$, we can further take a small $\bar{v}_n/\overline{E}$ expansion for $\alpha_1$ and $\alpha_2$. It can be shown that $\alpha_1$ and $\alpha_2$ then reduce to simple forms, $\alpha_1 \approx -\frac{8\overline{W}^2}{3\overline{E}^6}\cos(2\overline{E}d\cos\theta)$ and $\alpha_2 \approx \frac{8\overline{W}^2}{3\overline{E}^6}$. Thus, Eq. **13** gives the following expression for $\gamma$ in the limit $\overline{W} \ll \overline{E}$:

$$\gamma = \xi^{-1} \approx \frac{\overline{W}^2 \sin^4\theta}{12\overline{E}^2 d}\left[1 - \cos(2\overline{E}d\cos\theta)\right]. \qquad [14]$$

We also numerically calculated the localization length in this limit. The results are shown in Fig. 3*B* by the symbols. We find excellent agreement between the analytical and numerical results. We note that $\gamma$ vanishes at certain energies that satisfy the on-average Fabry–Perot resonance condition $\overline{E}d\cos\theta = m\pi$ ($m \in$ integers). Such Fabry–Perot resonance-induced anomalies were also observed in conventional 1D disordered materials (49–51). Thus, $\xi$ tends to diverge at these energies. The finite values of $\xi$ at these resonances are due to high-order corrections.

For pseudospin-1/2 systems, the asymptotic behavior of $\gamma$ in the limit of small $k_y$ and $\overline{W} \ll \overline{E}$ can be obtained using a similar approach (*Lyapunov Exponent in the Region of* $\overline{W} < \overline{E}$,) and has the expression

$$\gamma = \xi^{-1} \approx \frac{\overline{W}^2 \sin^2\theta}{12\overline{E}^2 d}\left[1 - \cos(2\overline{E}d\cos\theta)\right]. \qquad [15]$$

The validity of Eq. **15** is also confirmed numerically (Fig. S1). From Eqs. **14** and **15**, we can see that in both pseudospin systems the localization length decreases as $\xi \propto \overline{W}^{-2}$, showing exactly the same behaviors in Fig. 2. More importantly, our analytical results prove that the pseudospin number indeed makes a profound difference on the localization behaviors, leading to a $\xi \propto \sin^{-4S}\theta$ localization length behavior for small $\theta$, where $S$ is the pseudospin number.

**Asymptotic $\theta$-Dependent Localization Length Behavior in Region $\overline{W} > \overline{E}$.** In this case, there are strong scatterings for those layers with the potentials $\bar{v}$ close to the incident energy $\overline{E}$ due to the existence of singularity at $\overline{E} = \bar{v}$ in the scattering potential in Eq. **7**, and hence the approximations used above are not applicable. Although the calculation becomes rather tedious, we still manage to obtain an analytic form of $\gamma_2$ for pseudospin-1 systems (*$\gamma_2$ for Pseudospin-1 Systems in the Case* $\overline{W} > \overline{E}$); that is,

$$\gamma_2 \approx -\frac{1}{2d}\langle \ln|1 - r^2_{n,n-1}|\rangle_c \approx \frac{\overline{E}^2 \sin^2\theta}{2\overline{W}^2 d}. \qquad [16]$$

To confirm the validity of Eq. **16**, we numerically calculate $\gamma_2$ as a function of the incident angle for $\overline{W} = 0.03$ and $\overline{E} = 0.02$. The result is plotted by red circles in Fig. 4*A*, which agrees excellently with the analytic expression (red solid line) shown in Eq. **16**. Because the Lyapunov exponent, $\gamma = \gamma_1 + \gamma_2$, is an even function of $\sin\theta$, we can safely conclude from Eq. **16** that the region $\overline{W} > \overline{E}$ represents a different localization phase in which the $\theta$-dependent localization length has an asymptotic behavior, $\gamma = \xi^{-1} \propto \sin^2\theta$, different from the $\xi^{-1} \propto \sin^4\theta$ behavior found in the region $\overline{W} < \overline{E}$ as shown in Eq. **13**. Such a sudden change of $\theta$-dependent localization behavior at $\overline{W} = \overline{E}$ is accompanied by the cusp-like change of localization length from a decreasing function of $\overline{W}$ when $\overline{W} < \overline{E}$ to an increasing one when $\overline{W} > \overline{E}$ as shown in Fig. 2 *A* and *B*. We show in *$\gamma_2$ for Pseudospin-1 Systems in the Case* $\overline{W} > \overline{E}$ that the origin of the $\sin^2\theta$ factor in $\gamma_2$ is the occurrence of the diverging scattering potentials in certain layers when $|k_y| > |\overline{E} - \overline{U}(u)|$ so that the waves become evanescent inside these layers. In fact, the presence of evanescent waves in certain layers also leads to a $\sin^2\theta$ dependence in $\gamma_1$. Due to the complexity of the matrix $\hat{D}^0_{N+1}$, an explicit analytic expression for $\gamma_1$ is formidable. We numerically calculate $\gamma_1$ and plot the result by green triangles in Fig. 4*A*, which has an excellent fit to a dotted line showing $\gamma_1 \propto \sin^2\theta$. If the presence of evanescent waves is the origin that turns a $\sin^4\theta$ dependence of $\gamma$ into a $\sin^2\theta$ dependence, we should be able to recover the $\sin^4\theta$ behavior found in region $\overline{W} < \overline{E}$ by purposely excluding evanescent waves in the random media. To confirm this point, we calculate the $\theta$ dependence of $\gamma$ for a particular random distribution of potentials, $\bar{v} \in [-\overline{W}, \overline{W}]$, but with a condition $|\overline{E} - \bar{v}| > 0.1\overline{E}$ so that no evanescent waves will occur at sufficiently small $\theta$. The result is plotted by blue squares in Fig. 4*A*. It is clearly seen that the $\gamma \propto \sin^4\theta$ behavior is indeed recovered. In fact, the sudden drop of $\xi$ near $\overline{W}_c = \overline{E}$ shown in Fig. 2 *A* and *B* is also due to the presence of evanescent waves in some layers. To show this, we numerically calculate $\xi$ as a function of $\overline{W}$ by excluding the evanescent waves. The result is plotted by a blue dashed line in Fig. 4*B*. In comparison with the result with evanescent waves included (blue circles), we can see that the sudden drop of $\xi$ near $\overline{W}_c = \overline{E}$ disappears.

However, for pseudospin-1/2 systems, propagating waves also contribute to $\gamma$ a $\sin^2\theta$ term due to the interface scattering terms in Eq. **8**, which smears out the sudden drop of $\xi$, as shown in Fig. 2 *C* and *D*, and leads to the same asymptotic $\theta$ dependence of $\xi$ for all $\overline{W}$s in Fig. 3*A*.

## Conclusions

We discovered interesting anomalous localization behaviors in disordered pseudospin-1 systems, using the TMM as well as analytical solutions from the SGF method. In contrast to ordinary 1D random media where stronger randomness always induces stronger localization, pseudospin-1 systems have a critical random strength $\overline{W}_c = \overline{E}$ at which a cusp-like turnaround occurs in the localization length as a function of randomness. Additional randomness beyond this critical strength makes the wave less localized. Such a sudden change gives rise to two localization phases characterized by different asymptotic $\theta$ dependence of the localization length; i.e., $\xi \propto \sin^{-4}\theta$ when $\overline{W} < \overline{W}_c$ and $\xi \propto \sin^{-2}\theta$ when $\overline{W} > \overline{W}_c$. Such anomalous behaviors arise from the existence of a Dirac-like point and the occurrence of the evanescent waves in the region $\overline{W} > \overline{W}_c$. For pseudospin-1/2 systems, we find that the sharp transition is smeared out by additional interface scattering terms and the localization length behavior shows a smooth change from decreasing with the random strength at small $\overline{W}$ to increasing at large $\overline{W}$. In both regions, the $\theta$ dependence of $\xi$ follows the same asymptotic behavior $\xi \propto \sin^{-2}\theta$. Recently pseudospin-1 systems have been experimentally realized in photonic (25, 26, 34–37) and ultracold atom systems (33). Meanwhile, the applied potentials in such systems can be realized by uniformly scaling the structure in PCs (27) or manipulating an appropriate holographic mask in ultracold atom systems (28–32). Thus, it is experimentally feasible to prepare a 1D disordered pseudospin-1 system using such artificial structures. For a given randomness $W$, two localization phases can be observed by tuning the incident energy from $E > W$ to $E < W$.

**ACKNOWLEDGMENTS.** This work was supported by a grant from the Research Grants Council of Hong Kong (Project AoE/P-02/12). S.G.L. also acknowledges support from the National Science Foundation under Grant DMR-1508412.

1. Anderson PW (1958) Absence of diffusion in certain random lattices. *Phys Rev* 109:1492–1505.
2. Lee PA, Ramakrishnan TV (1985) Disordered electronic systems. *Rev Mod Phys* 57:287–337.
3. Sheng P (1990) *Scattering and Localization of Classical Waves in Random Media* (World Scientific, Singapore).
4. Soukoulis CM, Economou EN (1999) Electronic localization in disordered systems. *Waves Random Media* 9:255–269.
5. Kramer B, MacKinnon A (1993) Localization: Theory and experiment. *Rep Prog Phys* 56:1469–1564.
6. Schwartz T, Bartal G, Fishman S, Segev M (2007) Transport and Anderson localization in disordered two-dimensional photonic lattices. *Nature* 446:52–55.
7. Hsieh P, et al. (2015) Photon transport enhanced by transverse Anderson localization in disordered superlattices. *Nat Phys* 11:268–274.
8. Lahini Y, et al. (2008) Anderson localization and nonlinearity in one-dimensional disordered photonic lattices. *Phys Rev Lett* 100:013906.
9. Tian CS, Cheung SK, Zhang ZQ (2010) Local diffusion theory for localized waves in open media. *Phys Rev Lett* 105:263905.
10. John S, Sompolinsky H, Stephen MJ (1983) Localization in a disordered elastic medium near two dimensions. *Phys Rev B* 27:5592–5603.
11. Bloch I (2005) Ultracold quantum gases in optical lattices. *Nat Phys* 1:23–30.
12. Soukoulis CM, Kafesaki M, Economou EN (2006) Negative-index materials: New frontiers in optics. *Adv Mater* 18:1941–1952.
13. Novoselov KS, et al. (2004) Electric field effect in atomically thin carbon films. *Science* 306:666–669.
14. Castro Neto AH, Guinea F, Peres NMR, Novoselov KS, Geim AK (2009) The electronic properties of graphene. *Rev Mod Phys* 81:109–162.
15. Asatryan AA, et al. (2007) Suppression of Anderson localization in disordered metamaterials. *Phys Rev Lett* 99:193902.
16. Mogilevtsev D, Pinheiro FA, dos Santos RR, Cavalcanti SB, Oliveira LE (2010) Suppression of Anderson localization of light and Brewster anomalies in disordered superlattices containing a dispersive metamaterial. *Phys Rev B* 82:081105.
17. Torres-Herrera EJ, Izrailev FM, Markarov NM (2012) Non-conventional Anderson localization in bilayered structures. *Europhys Lett* 98:27003.
18. Choi SK, Park CH, Louie SG (2014) Electron supercollimation in graphene and Dirac Fermion materials using one-dimensional disorder potentials. *Phys Rev Lett* 113:026802.
19. Zhu SL, Zhang DW, Wang ZD (2009) Delocalization of relativistic Dirac particles in disordered one-dimensional systems and its implementation with cold atoms. *Phys Rev Lett* 102:210403.
20. Hasan MZ, Kane CL (2010) Colloquium: Topological insulators. *Rev Mod Phys* 82:3045–3067.
21. Qi XL, Zhang SC (2011) Topological insulators and superconductors. *Rev Mod Phys* 83:1057–1110.
22. Zhang X (2008) Observing Zitterbewegung for photons near the Dirac point of a two-dimensional photonic crystal. *Phys Rev Lett* 100:113903.
23. Sakoda K (2012) Dirac cone in two- and three-dimensional metamaterials. *Opt Express* 20:3898–3917.
24. Mei J, Wu Y, Chan CT, Zhang ZQ (2012) First-principles study of Dirac and Dirac-like cones in phononic and photonic crystals. *Phys Rev B* 86:035141.
25. Huang XQ, Lai Y, Hang ZH, Zheng H, Chan CT (2011) Dirac cones induced by accidental degeneracy in photonic crystals and zero-refractive-index materials. *Nat Mater* 10:582–586.
26. Moitra P, et al. (2013) Realization of an all-dielectric zero-index optical metamaterial. *Nat Photon* 7:791–795.
27. Fang A, Zhang ZQ, Louie SG, Chan CT (2016) Klein tunneling and supercollimation of pseudospin-1 electromagnetic waves. *Phys Rev B* 93:035422.
28. Shen R, Shao LB, Wang B, Xing DY (2010) Single Dirac cone with a flat band touching on line-centered-square optical lattices. *Phys Rev B* 81:041410.
29. Juzeliunas G, Ruseckas J, Dalibard J (2010) Generalized Rashba-Dresselhaus spin-orbit coupling for cold atoms. *Phys Rev A* 81:053403.
30. Urban DF, Bercioux D, Wimmer M, Hausler W (2011) Barrier transmission of Dirac-like pseudospin-one particles. *Phys Rev B* 84:115136.
31. Dora B, Kailasvuori J, Moessner R (2011) Lattice generalization of the Dirac equation to general spin and the role of the flat band. *Phys Rev B* 84:195422.
32. Xu Y, Jin G (2014) Omnidirectional transmission and reflection of pseudospin-1 Dirac fermions in a Lieb superlattice. *Phys Lett A* 378:3554–3560.
33. Taie S, et al. (2015) Coherent driving and freezing of bosonic matter wave in an optical Lieb lattice. *Sci Adv* 1:e1500854.
34. Guzman-Silva D, et al. (2014) Experimental observation of bulk and edge transport in photonic Lieb lattices. *New J Phys* 16:063061.
35. Mukherjee S, et al. (2015) Observation of a localized flat-band state in a photonic Lieb lattice. *Phys Rev Lett* 114:245504.
36. Vicencio RA, et al. (2015) Observation of localized states in Lieb photonic lattices. *Phys Rev Lett* 114:245503.
37. Diebel F, Leykam D, Kroesen S, Denz C, Desyatnikov AS (2016) Conical diffraction and composite Lieb bosons in photonic lattices. *Phys Rev Lett* 116:183902.
38. Xu HY, Lai YC (2016) Revival resonant scattering, perfect caustics, and isotropic transport of pseudospin-1 particles. *Phys Rev B* 94:165405.
39. Bliokh YP, Freilikher V, Savelev S, Nori F (2009) Transport and localization in periodic and disordered graphene superlattices. *Phys Rev B* 79:075123.
40. Abedpour N, Esmailpour A, Asgari R, Reza Rahimi Tabar M (2009) Conductance of a disordered graphene superlattice. *Phys Rev B* 79:165412.
41. Zhao Q, Gong J, Muller CA (2012) Localization behavior of Dirac particles in disordered graphene superlattices. *Phys Rev B* 85:104201.
42. McEuen PL, Bockrath M, Cobden DH, Yoon YG, Louie SG (1999) Disorder, pseudospins, and backscattering in carbon nanotubes. *Phys Rev Lett* 83:5098–5101.
43. Ando T, Nakanishi T, Saito R (1998) Berry's phase and absence of back scattering in carbon nanotubes. *J Phys Soc Jpn* 67:2857–2862.
44. Sipe JE, Sheng P, White BS, Cohen MH (1988) Brewster anomalies: A polarization-induced delocalization effect. *Phys Rev Lett* 60:108–111.
45. Bliokh KY, Freilikher VD (2004) Localization of transverse waves in randomly layered media at oblique incidence. *Phys Rev B* 70:245121.
46. Tworzydlo J, Trauzettel B, Titov M, Rycerz A, Beenakker CWJ (2006) Sub-poissonian shot noise in graphene. *Phys Rev Lett* 96:246802.
47. Sepkhanov RA, Bazaliy YB, Beenakker CWJ (2007) Extremal transmission at the Dirac point of a photonic band structure. *Phys Rev A* 75:063813.
48. Aronov AG, Gasparian VM, Gummich U (1991) Transmission of waves through one-dimensional random layered systems. *J Phys Condens Matter* 3:3023–3039.
49. Kappus M, Wegner F (1981) Anomaly in the band center of the one-dimensional Anderson model. *Z Phys B Con Mat* 45:15–21.
50. van Tiggelen BA, Tip A (1991) Photon localization in disorder-induced periodic multilayers. *J Phys I France* 1:1145–1154.
51. Crisanti A (1990) Resonances in random binary optical media. *J Phys A Math Gen* 23:5235–5240.